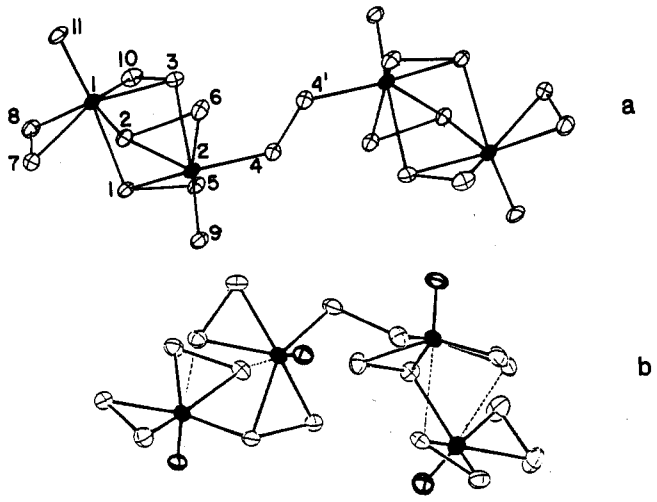

Figure 2. Structure of the $Nb_4Se_{22}^{6-}$ ion (a) in comparison to that of the $Mo_4S_{18}O_4^{2-}$ ion (b).[25]

reasonable yield two new chalcogenides of Ta and Nb: $K_4Ta_2S_{11}$ and $K_3Nb_2Se_{11}$. These contain the discrete anions $Ta_2S_{11}^{4-}$ and $Nb_4Se_{22}^{6-}$, which bear striking resemblances to closely related W and Mo species prepared by solution methods.

Transparent orange crystals and polycrystalline material of formula $K_4Ta_2S_{11}$ were prepared from the reaction among K_2S, Ta, and S (in 3:2:5 mole ratio) in a sealed evacuated quartz vessel that was kept at 800 °C for 48 h and then cooled at 100 °C/h. Electron microprobe analysis of the air- and moisture-sensitive crystals established their homogeneity and the presence of K, Ta, and S. The Guinier powder pattern suggested a novel structure type; i.e., lines for intercalated TaS_2 were not detected, nor was the K_3TaS_4-type structure. The presence of a TaS_4^{3-} unit was also ruled out by spectroscopic data since a characteristic IR band at 424 cm^{-1} was lacking. However, the spectroscopic data did suggest the presence of S_2^{2-} ligands, terminal Ta=S moieties, and Ta-bridging S^{2-} anions.[23] The structural details of the $Ta_2S_{11}^{2-}$ anion were determined by a single-crystal X-ray diffraction study on a thin translucent orange platelet of $K_4Ta_2S_{11}$.[24]

The crystal structure of $K_4Ta_2S_{11}$ consists of well-separated K^+ and $Ta_2S_{11}^{4-}$ ions (Figure 1a). The Ta···Ta distance of 3.442 (1) Å in the $Ta_2S_{11}^{4-}$ anion indicates no bonding between the Ta atoms. The Ta atoms are linked by one S^{2-} anion with an average Ta–S distance of 2.479 (5) Å and two S_2^{2-} ligands with average Ta–S and S–S distances of 2.579 (5) and 2.076 (7) Å, respectively. Each Ta atom is also bound to an additional S_2^{2-} ligand with average Ta–S and S–S distances of 2.465 (5) and 2.076 (9) Å, respectively. The coordination sphere of each Ta atom is completed by a short Ta=S interaction (average Ta–S distance = 2.235 (5) Å) to form a $Ta_2(\mu\text{-}S)(\mu\text{-}\eta^2,\eta^1\text{-}S_2)_2(\eta^2\text{-}S_2)_2(S)_2^{4-}$ anion with Ta in the 5+ oxidation state. This anion is closely related to the recently reported $[NEt_4]_2[Mo_2S_9O_2]$[25] complex prepared in solution; it contains the $Mo_2(\mu\text{-}S)(\eta^2\text{-}S_2)_4(O)_2^{2-}$ discrete anion (Mo, 6+) (Figure 1b). In contrast to the Ta species, each Mo atom shows only a weak intramolecular (rather than a bonding) interaction to a neighboring S_2^{2-} ligand. The $[PPh_4]_2[W_2S_{11}]$[8] complex, prepared by solution chemistry, provides another example of a similar anion, $W_2(\mu\text{-}S)(\eta^2\text{-}S_2)_4(S)_2^{2-}$.

$K_3Nb_2Se_{11}$ was prepared through the reaction of Nb metal with K_2Se and Se (in a 1:3:10 mole ratio) at 375 °C for 100 h with a 3 °C/h cooling rate to room temperature. Black chunky crystals were obtained upon dissolution of the excess melt with water. The structure was determined by single-crystal X-ray diffraction methods[26] after the homogeneity of the crystals and the presence of K, Nb, and Se were confirmed by electron microprobe analysis. The final formula, $K_3Nb_2Se_{11}$, was verified by quantitative analyses.

The crystal structure of $K_3Nb_2Se_{11}$ consists of well-separated K^+ and $Nb_4Se_{22}^{6-}$ ions. Within the $Nb_4Se_{22}^{6-}$ anion (Figure 2a) each nonbonding Nb pair (Nb···Nb distance = 3.679 (3) Å) is bridged by three Se_2^{2-} ligands with an average Nb–Se contact of 2.683 (3) Å and Se–Se interaction of 2.358 (3) Å. Each Nb atom is bound to a terminal Se anion to form a Nb–Se bond showing an average bond length of 2.361 (3) Å. The coordination sphere of the Nb atoms is completed by the addition of two Se_2^{2-} ligands (average Se–Se distance = 2.371 (4) Å) per Nb pair. One Se_2^{2-} ligand is bound to a Nb atom in a typical η^2-fashion while the second Se_2^{2-} links the other Nb atom to a neighboring dimer yielding a tetrameric anion best described as $[Nb_2(\mu\text{-}\eta^2,\eta^1\text{-}Se_2)_3(\eta^2\text{-}Se_2)(Se)_2]_2(\mu\text{-}\eta^1\text{-}Se_2)^{6-}$ with Nb in the 5+ oxidation state. This species is related to a soluble molybdenum oxysulfide, $[Et_4N]_2[Mo_4S_{18}O_4]$[25] (Mo, 6+) (Figure 2b). Again the major structural difference is related to the bridging $\eta^2,\eta^1\text{-}Q_2^{2-}$ ligands. In the Mo complex, the metal pairs are bridged by only one S_2^{2-} unit while the other two S_2^{2-} ligands show only weak intramolecular interaction yielding a $[Mo_2(\mu\text{-}\eta^2,\eta^1\text{-}S_2)(\eta^2\text{-}S_2)_3(O)_2]_2(\mu\text{-}\eta^1\text{-}S_2)^{2-}$ ion.

As evidenced by the structures of $K_4Ta_2S_{11}$ and $K_3Nb_2Se_{11}$, traditional solid-state synthesis provides a potentially useful route to new anionic chalcogenide species and possibly the only means to Nb and Ta analogues of Mo and W chalcogenide anions. The stability of these Nb and Ta anions in the solid-state can be exploited in an attempt to obtain isolated ions in solution for subsequent chemistry. The generation of quasi-isolated polyatomic Zintl,[27] polyarsenide,[28] and metal arsenide[29] anions has been achieved via the solubilization of their alkali-metal compounds. Presently, the solubilization of $K_4Ta_2S_{11}$ and $K_3Nb_2Se_{11}$ is being explored.

Acknowledgment. This work was supported by the U.S. National Science Foundation (Grant No. CHE-87-01007). Use was made of the Scanning Electron Microscope Facility of Northwestern University's Material Research Center, supported in part under the NSF-MRL program (Grant DMR-85-20280). S.S. acknowledges support under the NSF Summer Solid-State Program (Grant DMR-85-19905).

Supplementary Material Available: A listing of positional parameters (1 page). Ordering information is given on any current masthead page.

(23) IR (Nujol, CsI): Ta—S_2; ν(Ta—S), 331 (m), 319 (m), 301 (m) cm^{-1}; ν(S—S), 520 (m) cm^{-1}; ν(Ta=S), 505 (s) cm^{-1}; ν(Ta—S—Ta), 452 (s) cm^{-1}.

(24) Crystal data for $K_4Ta_2S_{11}$: orthorhombic, C_{2v}^5-$Pbc2_1$, $Z = 4$, $a = 7.409$ (3) Å, $b = 13.074$ (1) Å, $c = 17.881$ (3) Å, $V = 1732$ Å^3 at −166 °C; 1850 independent reflections measured out to 2θ(Cu Kα_1) = 75°; $R(F) = 0.049$ on 1790 reflections having $F_o^2 > 3\sigma(F_o^2)$.

(25) Coucouvanis, D.; Hadjikyriacou, A. *Inorg. Chem.* **1987**, *26*, 1-2.

(26) Crystal data for $K_3Nb_2Se_{11}$: monoclinic, C_{2h}^5-$P2_1/a$, $Z = 4$, $a = 25.70$ (1) Å, $b = 8.943$ (5) Å, $c = 7.877$ (5) Å, $\beta = 97.92$ (2)°, $V = 1793$ Å at −160 °C; 6263 independent reflections measured out to 2θ(Mo Kα_1) = 65°; $R(F) = 0.090$ on 3421 reflections having $F_o^2 > 3\sigma(F_o^2)$.

(27) Corbett, J. D. *Chem. Rev.* **1985**, *85*, 383-397 and references therein.

(28) Behn, C. H. E. *J. Am. Chem. Soc.* **1980**, *102*, 6036-6040.

(29) von Schnering, H.-G.; Wolf, J.; Weber, D.; Ramerez, R.; Meyer, T. *Angew. Chem., Int. Ed. Engl.* **1986**, *25*, 353-354.

Department of Chemistry
Northwestern University
Evanston, Illinois 60208

Serge Schreiner
Lorraine E. Aleandri
Doris Kang
James A. Ibers*

Received September 7, 1988

Bromide-Assisted Hydrogen Peroxide Disproportionation Catalyzed by Vanadium Bromoperoxidase: Absence of Direct Catalase Activity and Implications for the Catalytic Mechanism

Vanadium has been known for decades to be an essential element;[1] however, the first vanadium-containing enzymes, a bro-

(1) For recent reviews see: Chasteen, N. D. *Struct. Bonding* **1983**, *53*, 105. Boyd, D. W.; Kustin, K. *Adv. Inorg. Biochem.* **1984**, *6*, 311.

0020-1669/89/1328-0393$01.50/0

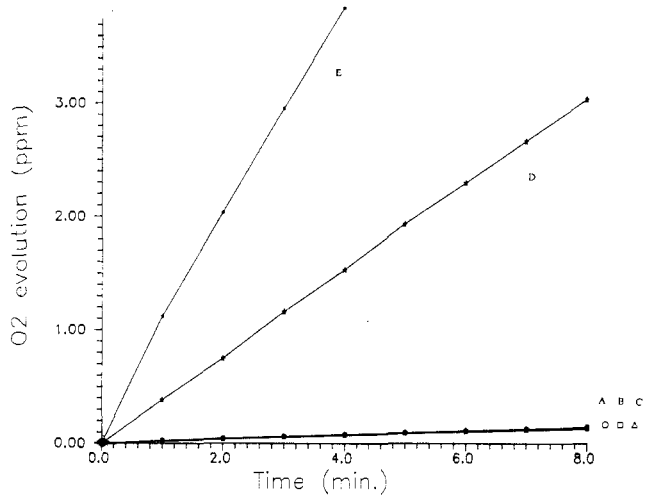

Figure 1. Halide-assisted disproportionation of hydrogen peroxide (dioxygen measurements made as described in Figure 2): (A) H_2O_2 (○); (B) H_2O_2 + 0.095 M KBr (□); (C) V-BrPO + H_2O_2 (△); (D) V-BrPO + H_2O_2 + 0.095 M KBr (☆); (E) V-BrPO + H_2O_2 + 0.095 M KI (*). All solutions were 2 mM H_2O_2 in 0.095 M phosphate buffer (pH 6.5). The enzyme concentration is 50 ng/mL on the basis of the Bio-Rad protein assay using bovine plasma albumin as the standard. The O_2 formation rate for V-BrPO + H_2O_2 was followed for at least 40 min with no change in the rate observed in (C).

moperoxidase[2,3] and a nitrogenase,[4,5] have only been discovered very recently. Vanadium bromoperoxidase (V-BrPO) was first isolated from the marine alga *Ascophyllum nodosum* and found to catalyze the bromination of monochlorodimedone (MCD) using hydrogen peroxide as an oxidant.[6] Bromoperoxidase enzymes are well-known in marine organisms, including Fe^{III}Heme-BrPO[7,8] and the recently discovered non-heme iron(III)-containing bromoperoxidase (Fe_{NH}-BrPO).[9] While all the bromoperoxidases are similar, particularly in the nature of substrates brominated (e.g., β-diketones, β-keto acids, phenols, etc.),[10] FeHeme-BrPO differs significantly from V-BrPO in the overall reaction chemistry catalyzed. We report below that unlike the FeHeme haloperoxidases (including BrPO and chloroperoxidase), which catalyze the disproportionation of hydrogen peroxide (i.e., "direct catalase" activity)[7,11]

$$2H_2O_2 \rightarrow O_2 + 2H_2O$$

V-BrPO *only* catalyzes the disproportionation of H_2O_2 in the presence of Br^- or I^-. We also report that the rate of dioxygen formation in the bromide-assisted catalase reaction is equal to the rate of MCD bromination, suggesting that both reactions proceed through a common intermediate, the production of which is rate-limiting. Moreover, while V-BrPO does not utilize H_2O_2 in the absence of bromide or iodide, neither does H_2O_2 inactivate the enzyme.

While the role of the FeHeme moiety in bromoperoxidase activity has been shown to be an electron-transfer catalyst proceeding through $Heme^+Fe^{IV}{=}O$,[7] the role of vanadium in V-BrPO is not yet known. V-BrPO is characterized by a single V(V) ion per subunit, which can be removed by dialysis at low pH against EDTA, rendering the enzyme inactive.[2,3] The bromoperoxidase activity can be fully restored only after recoordination of vanadate,[2] and aqueous vanadate does not function as a catalyst. The vanadyl BrPO derivative does not catalyze the bromination of MCD,[3] nor is a VO^{2+} ESR signal observed during turnover,[12] suggesting that the one-electron-reduced state of V^V-BrPO is not in the catalytic cycle.

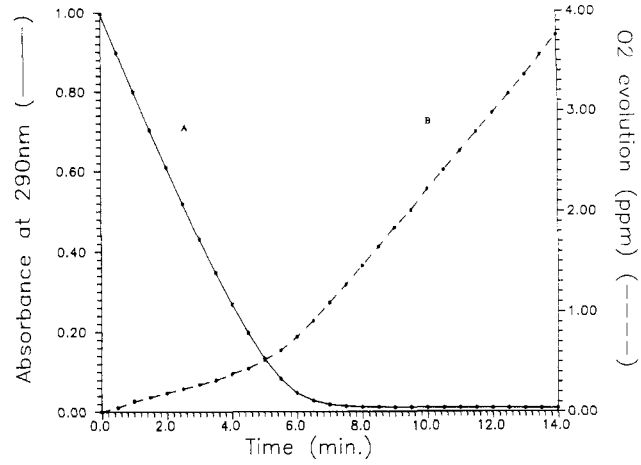

Figure 2. Inhibition of dioxygen formation during MCD bromination (reactions initiated by addition of H_2O_2 (final concentration 2 mM) to 0.095 M phosphate buffer (pH 6.5), 0.095 M KBr, 47.5 μM MCD, and 50 ng/mL V-BrPO at 25 °C): (A) bromination of MCD monitored at 290 nm (—); (B) O_2 formation measured with a YSI Clark-type dioxygen electrode in the presence of MCD as described (- - -). O_2 electrode measurements were made on N_2-sparged solutions. V-BrPO was isolated and purified from *A. nodosum* according to the published procedures.[6,14]

Table I[a]

[MCD], μM	$d[O_2]/dt$ during[b,d] MCD bromination, μM/min	$-d[MCD]/dt$[b]	$d[O_2]/dt$ after[b-d] MCD bromination, μM/min
0			10.4
40	2.0 (0.8)	10.2 (0.2)	10.1 (0.7)
50	1.3 (0.1)	10.8 (0.1)	9.9 (0.3)
70	1.0 (0.2)	10.4 (0.3)	10.3 (0.2)
95	0.5 (0.1)	10.7 (<0.1)	9.8 (0.6)
av		10.5 (0.5)	10.0 (0.3)

[a] All rates are an average of three determinations with the standard deviation given in parentheses. While the absolute magnitudes of the rates of MCD bromination and dioxygen formation vary with storage and the age of the enzyme, the ratio of $-d[MCD]/dt$ to $d[O_2]/dt$ still remains 1. The assay buffer is described in the caption of Figure 2. [b] The MCD bromination rates and the O_2 formation rate during bromination are reported for the first 10% of reaction. [c] Reported rate is obtained from the steepest slope of O_2 ppm vs time plot. [d] O_2 evolution rates are corrected for the instability of H_2O_2 (i.e., Figure 2A), which is <10% of the maximum O_2 rate observed.

Figure 1 shows that V-BrPO does *not* catalyze the direct disproportionation of hydrogen peroxide (Figure 1C), which is in distinct contrast to the case for the FeHeme haloperoxidases.[7] Addition of bromide, however, initiates rapid dioxygen evolution, which ceases when the hydrogen peroxide is completely consumed, indicating bromide-assisted catalase activity (Figure 1D).[13] Iodide assists the catalase reaction more efficiently than bromide (24.3 μM O_2 evolved/min at 0.95 mM I^- (Figure 1E) vs 10.4 μM

(2) Vilter, H. *Phytochemistry* **1984**, *23*, 1387.
(3) de Boer, E.; Boon, K.; Wever, R. *Biochemistry* **1988**, *27*, 1629.
(4) Morningstar, J. E.; Johnson, M. K.; Case, E. E.; Hales, B. J. *Biochemistry* **1987**, *26*, 1795. Hales, B. J.; Case, E. E.; Morningstar, J. E.; Dzeda, M. F.; Mauterer, L. A. *Biochemistry* **1986**, *25*, 7251.
(5) Robson, R. L.; Eady, R. R.; Richardson, T. H.; Miller, R. W.; Hawkins, M.; Postgate, J. R. *Nature* **1986**, *322*, 388.
(6) Wever, R.; Plat, H.; de Boer, E. *Biochim. Biophys. Acta* **1985**, *830*, 181.
(7) Manthey, J. A.; Hager, L. P. *J. Biol. Chem.* **1981**, *256*, 11232.
(8) Theiler, R. F.; Siuda, J. S.; Hager, L. P. In *Food and Drugs from the Sea*; Kaul, P. N., Sinderman, C. J., Eds.; University of Oklahoma Press: Norman, OK, 1978, pp 153–169.
(9) (a) Itoh, N.; Izumi, Y.; Yamada, H. *Biochemistry* **1987**, *26*, 282. (b) Itoh, N.; Izumi, Y.; Yamada, H. *J. Biol. Chem.* **1987**, *262*, 11982.
(10) For a review see: Neidleman, S. L.; Geigert, J. *Biohalogenation*; Ellis Horwood: 1986; and references therein.
(11) (a) Thomas, J. A.; Morris, D. R.; Hager, L. P. *J. Biol. Chem.* **1970**, *245*, 3129. (b) Araiso, T.; Rutter, R.; Palcic, M. M.; Hager, L. P.; Dunford, H. B. *Can. J. Biochem.* **1981**, *59*, 233.
(12) de Boer, E.; van Kooyk, Y.; Tromp, M. G. M.; Plat, H.; Wever, R. *Biochim. Biophys. Acta* **1986**, *869*, 48.
(13) Bromide is indeed a catalyst of hydrogen peroxide disproportionation as confirmed by monitoring the Br^- concentration with a bromide-selective electrode. The bromide concentration decreases to a steady-state concentration during turnover and returns to its initial concentration when the peroxide is consumed.

O_2/min at 0.095 M Br^-), reflecting the larger oxidation potential of iodide. Figure 1B shows that a solution of H_2O_2 and Br^- at pH 6.5 does not produce O_2, despite the favorable potential, and Figure 1A demonstrates that a solution of H_2O_2 is stable with respect to disproportionation under the conditions of these experiments.

Figure 2 shows a profile of the rate of MCD bromination (Figure 2A) and the rate of dioxygen formation (Figure 2B), both in the presence of 47.5 μM MCD catalyzed by V-BrPO. The rate of dioxygen formation catalyzed by V-BrPO, 10.0 μM/min, is identical with the rate of MCD bromination, 10.5 μM/min at 40–95 μM [MCD] (see Table I). Moreover, the maximum rate of O_2 formation is independent of the presence of MCD, since the rate of O_2 formation in the absence of MCD is 10.4 μM/min. That the ratio of the rate of MCD bromination to dioxygen formation is 1.05 ± 0.05 suggests that both reactions proceed through a common intermediate, which in analogy to FeHeme-BrPO may be an enzyme-bound OBr^- moiety, an enzyme-bound Br moiety, HOBr, or Br_3^-. Any of these can react with MCD to give the brominated product or with another 1 equiv of H_2O_2 to produce O_2 and Br^- at rates much faster than that for the production of the intermediate.[7,10,14,15] Chloride (≤0.5 M) does not affect the rate of MCD bromination nor the O_2-formation rate, although fluoride inhibits both reactions.

This is the first report of halide-dependent catalase activity for V-BrPO. This feature is shared with Fe_{NH}-BrPO, which is reported to have equivalent rates of MCD bromination and oxygen evolution in the halide-dependent catalase reaction,[9] but is distinctly different from the FeHeme haloperoxidases and many other FeHeme peroxidases, which have appreciable catalase activities in the absence of halide ion.[7,11] The identical rates of MCD bromination and Br^--assisted O_2 formation and the lack of O_2 formation in the absence of bromide suggest the possible mechanism

$$H_2O_2 + Br^- \xrightarrow{\text{V-BrPO}} \text{"intermediate"} \text{ (i.e., HOBr, } Br_3^-\text{, Enz-OBr, or Enz-Br)}$$

$$\text{"intermediate"} \xrightarrow{k_1[MCD]} \text{Br-MCD}$$

$$\text{"intermediate"} \xrightarrow{k_2[H_2O_2]} O_2 + Br^- + H_2O$$

During the bromination of MCD, a slow rate of O_2 formation is evident in Figure 2B, although, this rate is 80–95% less than the rate of O_2 formation in the absence of MCD or after all MCD is consumed. Even at much higher MCD concentrations (i.e., up 250 μM), the rate of O_2 formation is not completely shut off, indicating that k_1[MCD] competes with $k_2[H_2O_2]$ for reaction with the "intermediate". V-BrPO also catalyzes the bromination of uracil or cytosine, forming the 5-bromo derivatives,[16] although neither uracil nor cytosine is an efficient substrate, even at 10 mM concentrations, since dioxygen evolution (i.e., $k_2[H_2O_2]$) is concomitant with bromination (i.e., k_1[pyrimidine]).

In conclusion, we have shown that, unlike FeHeme haloperoxidases, V-BrPO cannot catalyze the direct disproportionation of H_2O_2 in the absence of bromide or iodide. The catalase activity of FeHeme haloperoxidases may be a consequence of the electron-transfer function of the FeHeme moiety since $Heme^+Fe^{IV}{=}O$ can oxidize H_2O_2, leading to direct catalase activity, or oxidize Br^-, leading to bromination and Br^--assisted catalase reactivity. We are continuing our investigation of the role of the vanadium(V) ion to determine whether V-BrPO functions as an electron-transfer catalyst or a Lewis acid catalyst of bromide oxidation by hydrogen peroxide.

Abbreviations: 2-chloro-5,5-dimethyl-1,3-dimedone, MCD; bromoperoxidase, BrPO; chloroperoxidase, ClPO.

Acknowledgment. A.B. gratefully acknowledges grants from the National Science Foundation (DMB87-16229), the donors of the Petroleum Research Fund, administered by the American Chemical Society, the Committee on Research of the UCSB Academic Senate, and the American Cancer Society, Junior Faculty Research Award (JFRA-216).

Department of Chemistry
University of California
Santa Barbara, California 93106

Richard R. Everett
Alison Butler*

Received September 14, 1988

(14) Kanofsky, J. R. *J. Biol. Chem.* **1984**, *259*, 5596.
(15) Griffin, B. W. *Biochem. Biophys. Res. Commun.* **1983**, *116*, 873.
(16) Formation of 5-bromocytosine was confirmed by electron impact mass spectral analysis and by comparison of R_f values from thin-layer chromatography.

General Synthetic Route to the Dirhenium Octahydrides $Re_2H_8(PR_3)_4$ from the Triply Bonded Complexes $Re_2Cl_4(PR_3)_4$. An Unexpected Structure for the Complex $Re_2H_8(dppm)_2$ (dppm = $Ph_2PCH_2PPh_2$)

The so-called "agno-hydrides" of rhenium were first described in detail by Chatt and Coffey in 1969 and formulated as $[ReH_x(PR_3)_2]_2$ ($x < 7$ and $PR_3 = PEt_2Ph$, PPh_3).[1] Later work by Bau et al.[2] identified these complexes as having the novel hydrido-bridged structure $Re_2(\mu\text{-}H)_4H_4(PR_3)_4$. The most commonly used method for the synthesis of these complexes and the more recently prepared dimethylphenylphosphine derivative $Re_2H_8(PMe_2Ph)_4$[3] involves the thermal decomposition of the corresponding mononuclear heptahydride complexes $ReH_7(PR_3)_2$ (i.e., the original Chatt and Coffey procedure).[4-8] Subsequently, the isolation of $Re_2H_8(PMe_3)_4$ has been reported,[9] although its synthesis involves a different recipe. In view of the novel chemistry that is now being uncovered for dirhenium polyhydride complexes,[10-13] we have sought to devise a simple synthetic methodology that would be suitable for an extensive range of phosphine ligands and so provide a single uniform synthetic strategy for $Re_2H_8(PR_3)_4$. We can now report the successful development of such a route for PR_3 = PMe_3, PEt_3, P-*n*-Pr_3, PMe_2Ph, PEt_2Ph, $PMePh_2$, $Ph_2PCH_2PPh_2$ (dppm), and $Ph_2PCH_2CH_2PPh_2$ (dppe)

(1) Chatt, J.; Coffey, R. S. *J. Chem. Soc. A* **1969**, 1963.
(2) Bau, R.; Carroll, W. E.; Teller, R. G.; Koetzle, T. F. *J. Am. Chem. Soc.* **1977**, *99*, 3872.
(3) Green, M. A. Ph.D. Thesis, Indiana University, 1982. This source provides details of the synthesis of $Re_2H_8(PMe_2Ph)_4$, a complex whose chemistry has been examined in detail by Professor K. G. Caulton and his group.
(4) An excellent alternative high-yield synthesis of $Re_2H_8(PPh_3)_4$ involves the reaction of the quadruply bonded dirhenium(III) complexes (n-$Bu_4N)_2Re_2Cl_8$ or $Re_2Cl_6(PPh_3)_2$ with $NaBH_4$ and PPh_3 in ethanol.[5] The photolysis of $ReH_5(PR_3)_3$ and $ReH_7(PR_3)_2$ (PR_3 = PPh_3, $PMePh_2$, PMe_2Ph) gives $Re_2H_8(PR_3)_4$, along with other products,[6,7] while the chemical oxidation of anionic $K[ReH_6(PMePh_2)_2]$ leads to $Re_2H_8(PMePh_2)_4$.[8] However, these latter reactions have not yet been developed into useful synthetic procedures.
(5) Brant, P.; Walton, R. A. *Inorg. Chem.* **1978**, *17*, 2674.
(6) Green, M. A.; Huffman, J. C.; Caulton, K. G. *J. Am. Chem. Soc.* **1981**, *103*, 695.
(7) Roberts, D. A.; Geoffroy, G. L. *J. Organomet. Chem.* **1981**, *214*, 221.
(8) Bruno, J. W.; Caulton, K. G. *J. Organomet. Chem.* **1986**, *315*, C13.
(9) Lyons, D.; Wilkinson, G. *J. Chem. Soc., Dalton Trans.* **1985**, 587.
(10) Green, M. A.; Huffman, J. C.; Caulton, K. G. *J. Am. Chem. Soc.* **1982**, *104*, 2319.
(11) (a) Allison, J. D.; Walton, R. A. *J. Am. Chem. Soc.* **1984**, *106*, 163. (b) Allison, J. D.; Cotton, F. A.; Powell, G. L.; Walton, R. A. *Inorg. Chem.* **1984**, *23*, 159.
(12) (a) Boyle, P. D.; Johnson, B. J.; Alexander, B. D.; Casalnuovo, J. A.; Gannon, P. R.; Johnson, S. M.; Larka, E. A.; Mueting, A. M.; Pignolet, L. H. *Inorg. Chem.* **1987**, *26*, 1346. (b) Moehring, G. A.; Fanwick, P. E.; Walton, R. A. *Inorg. Chem.* **1987**, *26*, 1861.
(13) (a) Rhodes, L. F.; Huffman, J. C.; Caulton, K. G. *J. Am. Chem. Soc.* **1983**, *105*, 5137. (b) Sutherland, B. R.; Ho, D. M.; Huffman, J. C.; Caulton, K. G. *Angew. Chem., Int. Ed. Engl.* **1987**, *26*, 135. (c) Westerberg, D. E.; Sutherland, B. R.; Huffman, J. C.; Caulton, K. G. *J. Am. Chem. Soc.* **1988**, *110*, 1642.

0020-1669/89/1328-0395$01.50/0